51. IWK

Internationales Wissenschaftliches Kolloquium
International Scientific Colloquium

PROCEEDINGS 11-15 September 2006

FACULTY OF ELECTRICAL ENGINEERING AND INFORMATION SCIENCE

INFORMATION TECHNOLOGY AND ELECTRICAL ENGINEERING - DEVICES AND SYSTEMS, MATERIALS AND TECHNOLOGIES FOR THE FUTURE

Startseite / Index:
http://www.db-thueringen.de/servlets/DocumentServlet?id=12391

TECHNISCHE UNIVERSITÄT
ILMENAU

Impressum

Herausgeber: Der Rektor der Technischen Universität Ilmenau
Univ.-Prof. Dr. rer. nat. habil. Peter Scharff

Redaktion: Referat Marketing und Studentische Angelegenheiten
Andrea Schneider

Fakultät für Elektrotechnik und Informationstechnik
Susanne Jakob
Dipl.-Ing. Helge Drumm

Redaktionsschluss: 07. Juli 2006

Technische Realisierung (CD-Rom-Ausgabe):
Institut für Medientechnik an der TU Ilmenau
Dipl.-Ing. Christian Weigel
Dipl.-Ing. Marco Albrecht
Dipl.-Ing. Helge Drumm

Technische Realisierung (Online-Ausgabe):
Universitätsbibliothek Ilmenau
ilmedia
Postfach 10 05 65
98684 Ilmenau

Verlag:
Verlag ISLE, Betriebsstätte des ISLE e.V.
Werner-von-Siemens-Str. 16
98693 Ilrnenau

ISBN (Druckausgabe): 3-938843-15-2
ISBN (CD-Rom-Ausgabe): 3-938843-16-0

Startseite / Index:
http://www.db-thueringen.de/servlets/DocumentServlet?id=12391

51st Internationales Wissenschaftliches Kolloquium
Technische Universität Ilmenau
September 11 – 15, 2006

B. Hamann / J. Schawohl / C. Kraffert

Large Hexaferrite Single Crystals Grown in a DC Magnetic Field

Abstract

For the production of barium and strontium hexaferrite different technologies are known. Hexaferrites for industrial application of commodities are manufactured by ceramic technologies. For special application and scientific purposes the glass crystallization technology is being used. Since the middle of 2005 the authors have been working on a further technology, the crystallization from melts of the system BaO-B_2O_3-Fe_2O_3. This crystallization is carried out at temperatures between 1,200 °C and 400 °C and takes place in a DC magnetic field at a flux density of 5 Tesla. After separation of the hexaferrites from the borate matrix single crystals with edge lengths up to 5 mm and crystal thickness up to 0.6 mm are obtained. Furthermore the used equipment is presented, the analysis of the crystal characteristics is described and material properties of the crystals are indicated.

1. Introduction

The existing results are part of the work of the Junior Research Group “Electromagnetic Processing of Materials” (EPM) at the Technical University of Ilmenau. The studies about crystallizing barium hexaferrite from a melt were started in autumn 2005. Based on a molar composition of 39.6 BaO – 35.4 B_2O_3 – 25 Fe_2O_3 widely investigated for the crystallization of glass [1], initial exploratory experiments will be characterized, which were carried out in a DC magnetic field with a flux density of 5 Tesla. The objective is to publish the results in material development as well as to present the equipment used.

Hexaferrites are the most common magnetic materials. In 1985 the production

reached an average of 110,000 t worldwide and is increasing continuously. For the year 2010 a volume of a million t is expected [2].

The use of ferrites is most versatile and contains simple toys as well as high tech applications. Hexaferrites are easily to distinguish from other permanent magnets because of their black coloration. They consist of barium hexaferrite ($BaFe_{12}O_{19}$; BHF) or strontium hexaferrite ($SrFe_{12}O_{19}$). Table 3 also contains magnetic properties of both industrially manufactured types of ferrites. Because of its higher field intensity strontium hexaferrite is used for most applications. There is no significant difference in there production. Basic raw materials are barium or strontium carbonates, iron oxide and dopants. This mixture is calcinated in rotary klins with controlled atmospheres. After crushing hexaferrite crystals with grain sizes of 0.8 to 1.1 µm are ready for forming and sintering.

A second technology used in Ilmenau for a long time is the glass crystallization technique [3]. At first glass compositions of the system BaO-B_2O_3-Fe_2O_3 are melted and amorphizised. In the originated glass flakes, BHF crystals are generated through tempering, which are being separated chemically from the rest of the matrix. These BHF crystals have grain sizes between 50 and 500 nm and feature excellent hardmagnetic qualities. The sample Ha-N in table 1 represents such a material of the authors.

Furthermore it is known, that BHF can be made by crystallization from a melt. This technology is less established und was only analysed without magnetic fields. Extensive research working on this topic were accomplished by [4].

2. The Structure of Barium Hexaferrite Crystals

A systematic and comprehensive analysis of the physical and chemical properties of crystallized materials requires the availability of large, high quality crystals. Growing and characterizing them are the most important tasks in developing new materials for technological applications. Improving the technological relevant features of a crystal-

line material requires an in-depth knowledge of the properties, including the defects (real structure) of the monocrystalline material at all times.

Most materials, like metals, ceramics as well as semi-crystalline polymers are built up in a polycrystalline way. A quantitative comprehension of the properties of such materials has to start from the crystal structure and the features of the single crystals. Since the polycrystalline structure with its statistic distribution function of size, form and assembly (structure parameters) as well as the crystallographic orientation (texture parameter) has to be characterized, X-ray diffractions methods are being used to analyse it.

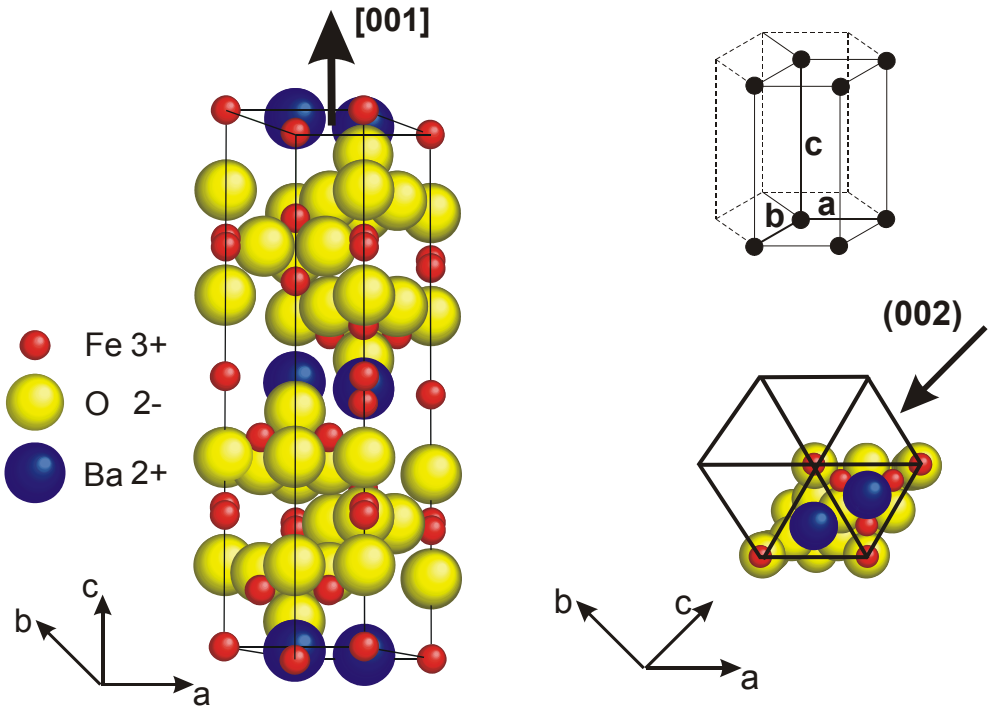

Figure 1 Unit cell of hexagonal $BaFe_{12}O_{19}$

BHF crystals feature a hexagonal structure like magnetoplumbite with a space group $P6_3/mmc$, see figure 1. The lattice parameters of the hexagonal unit cell with its three-dimensional periodic alignment of modules are a = 0.58920 and c = 2.3183 nm. Altogether, the unit cell contains 56 ions of the elements Ba, Fe and O. In c-direction the bariumhexaferrite crystal features a disproportional elongation.

3. Crystallization of Barium Hexaferrite in the Melt

3.1 Equipment

For processing glass melts in high magnetic fields a special equipment is used. It consists of two essential components, a cryogen free magnet (CFM), fabricated by Cryogenic Ltd. London and a high temperature furnace, fabricated by Xerion - Advanced Heating Freiberg.

The most important component is the CFM, that provides a DC magnetic field with a flux density differing between the earth magnetic field (0.00005 Tesla) and 5 Tesla. The CFM operates with a supra conducting coil of NbTi. In order to generate the supra conductivity it is necessary to run the coil at temperatures of around 4 K. This is reached which the 4K-Cryocooler, a cryogen-free cooling system from Sumitomo. The magnetic flux density is controlled by the power supply. That controls the current of the coil and thus the magnetic flux density. After achieving the chosen magnetic flux density the coil can be uncoupled from the power supply. The provided magnetic field is stable over weeks (persistent mode). For experimental investigations the CFM is tiltable, so that the work space (diameter 300 mm, height 400 mm) can be used in vertical and horizontal positions at room temperature.

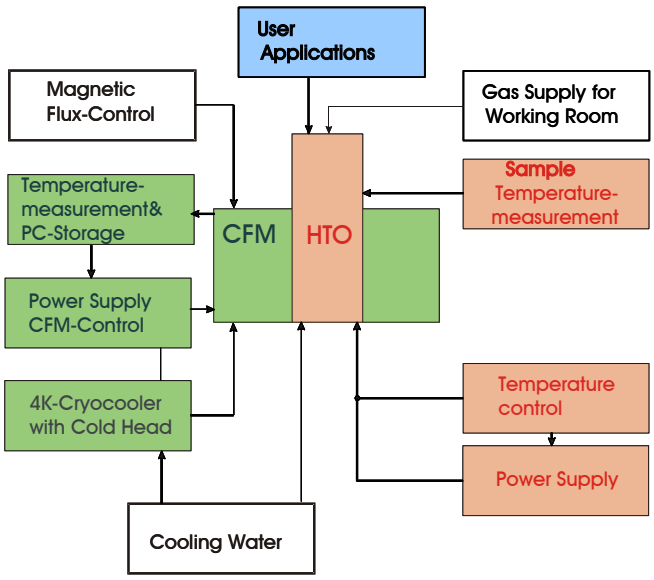

Scheme of operation between the units

Cryogen free 5T-DC-magnet with high temperature furnace

Figure 2 High field and high temperature equipment used for material investigations

For our high temperature investigations the CFM had been equipped with a specially designed high temperature furnace (HTO). This facility allows temperatures of 1,500 °C for long periods of time. The diameter of the working room is 50 mm and the usable height is up to 100 mm. The positions of CFM and HTO were assembled in such a way, that the maximum of temperature is on the same position like the maximum of the magnetic field. The characteristics of the curves in figure 3 and 4 show the distribution of field and temperature in the centre of the HTO.

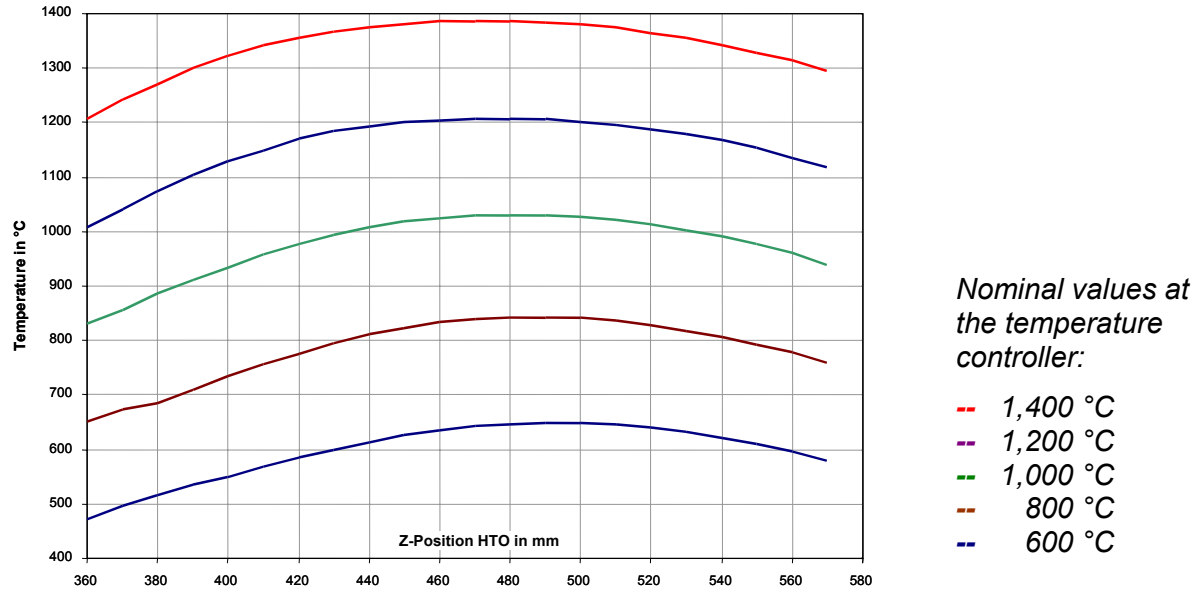

Figure 3 Characteristics of temperature in the HTO

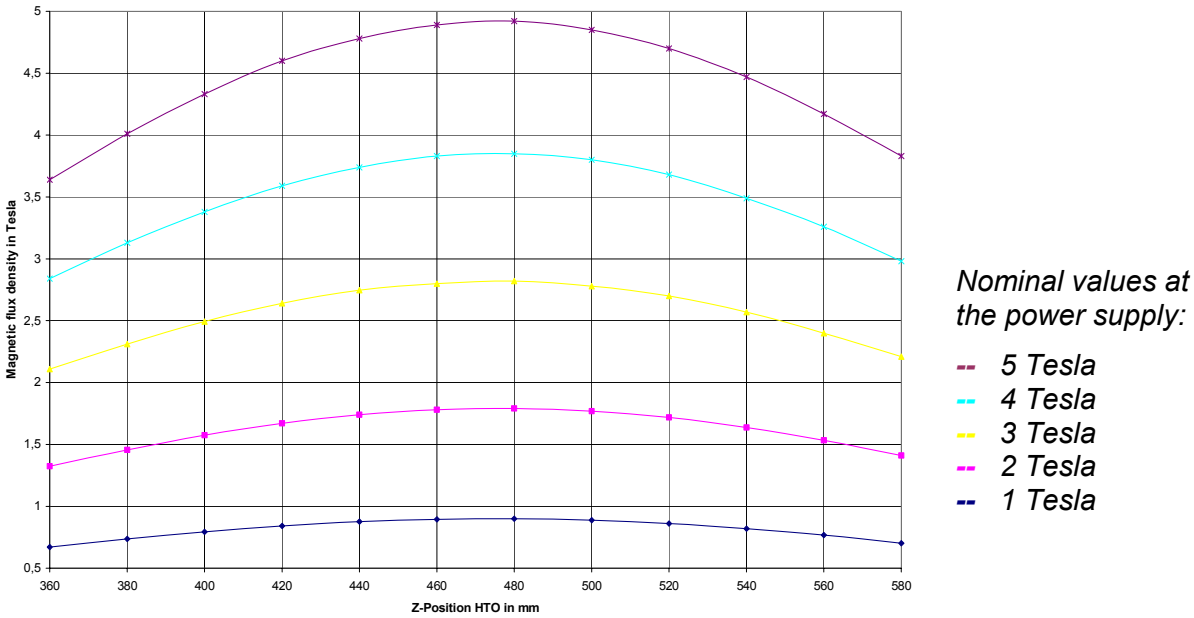

Figure 4 Distribution of magnetic flux density in the HTO

The equipment is additionally completed with a gas supply for working with defined atmospheres of Ar, CO/CO_2, O_2 and air. The hole system is quickly configurable and universally applicable for academic and industrial applications. You can find further information to the system and applications in [5].

3.2 Melt, Crystallization and Separation

For all experiments melts consisting of 39.6 mol% BaO, 35.4 mol% B_2O_3 and 25 mol% Fe_2O_3 were used. For each sample a new melt with a mass of 100 g was melted. For it the raw materials boric acid (>99.8 %, for analysis), barium carbonate (>99 %) and iron (III)-oxide were mixed for the batches of the melts. For the samples K3-N, Ha3 und Ha-N we used an iron oxide with a content of 97.8 ma% Fe_2O_3, all the other samples were prepared with an iron oxide for anlysis (content of Fe_2O_3: >99.8 %). In the samples K3-N and Ha-N $BaNO_3$ was used instead of 3.8 mass% $BaCO_3$ to increase the amount of oxygen in the melt (the extension "-N" stands for nitrate).

Table 1 Overview about the prepared samples, the crystallization processes and first visual results

sample code	tempering procedure			results and comments
	temperature range °C	cooling speed K/min	duration min	
K3-N	1,400 → 20	--	< 1	rapidly quenched glass; flakes
Ha3-F	1,200 → 1,100	0.33	303	liquid material
Ha3	1,200 → 1,100	0.33	303	solid material
HaFe4	1,200 → 1,100	0.1	1,000	solid material
HaFe5	1,200 → 800	0.1	4,000	sample completely solid
HaFe8	1,200 → 400	0.1	8,000	sample completely solid
Ha-N	constant at 850	0	1,800	crystallized flakes

The batches were melted in an electrically heated laboratory furnace with Pt-crucibles at a temperature of 1,400 °C. After a melting time of 1h for each sample, the crucibles were taken out of the furnace and cooled to room temperature by air.

Figure 5 shows the thermoanalytic (DSC) and the graphymetric (TG) behaviour of the melt while cooling from 1,400 to 200 °C. The DSC shows a minor exothermic reaction in the melt at 1,147 °C and a distinct exothermic peak at 716 °C. In the temperature range between 1,400 and 1,100 °C there is a nearly linear mass growth of 0.084 % per 100 K. At a temperature of 846 °C the maximum of mass growth will be reached. For the range between 1,400 to 846 °C the total growth is 0.36 %. Provided that the mass growth is caused by the oxidation of FeO to Fe_2O_3 at least 1.4 % FeO is included in the whole melt or 4.5 % of Fe_2O_3 exist as FeO.

The exothermic reaction at 1,147 °C can be associated with the crystallization of BHF. Through specific cooling of sample Ha3 between 1,200 and 1,100 °C $BaFe_{12}O_{19}$ is segregated as the only crystal phase watched.

For the second very distinct exothermic reaction at 716 °C no reaction could be associated yet. As the mass growth is completed, it is not an oxidation but another crystallization or a phase change reaction.

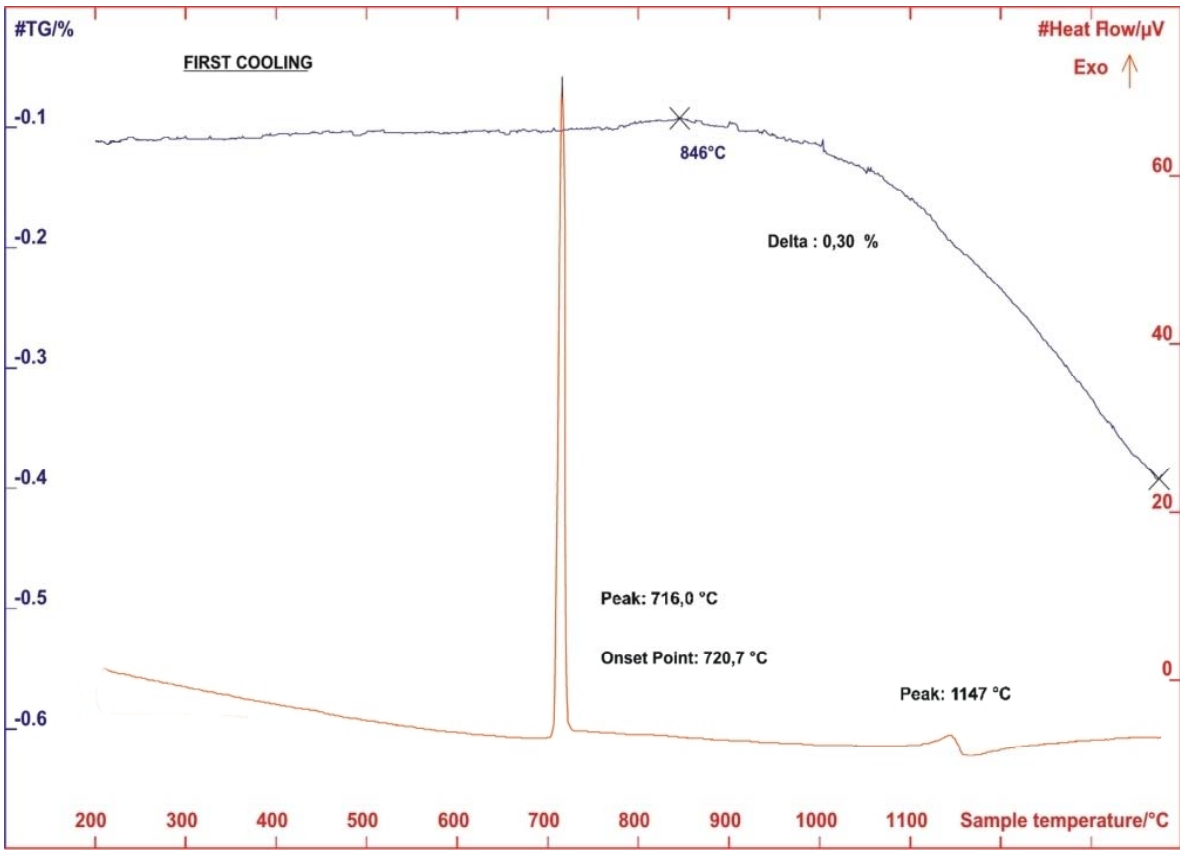

Figure 5 DSC and TG plot for melts with the molar composition of 39.6 BaO - 35.4 B_2O_3 -25.0 Fe_2O_3 (mass 113,38 mg, cooling rate 5 K/min)

The crucibles with melts Ha3, HaFe4, HaFe5 and HaFe8 were melted a second time in the high temperature furnace of CFM within a permanent DC magnetic field (flux density 5 Tesla) at a temperature of 1,400 °C for a time of 1h. Afterwards the samples were cooled considering the specifications in table 1. After reaching the final temperatures the crucibles were taken out of the HTO. The remaining melt of the samples Ha3 and HaFe4 were separated from the solid part by (hot) decanting. HaFe5 and HaFe8 were completely solid. The solid material remaining in the crucible was drilled out. To separate the BHF crystals the drill core had to be crushed and cooked in boiling diluted acetic acid. Because of this treatment (chemical separation according to [6]) the matrix dissolves and you will get separated BHF crystals. It was necessary to work with flexible solution times during this procedure because the matrix between close-by disc shaped crystals is much harder to dissolve than the one from crystallized flakes of sample Ha-N.

The crystals generated in the melt have variable dimensions. Figure 6 shows large crystals of the melt Ha3 remaining in the crucible which obtained dimensions up to 5 mm edges lengh in the square direction and with thicknesses up to 45 µm.

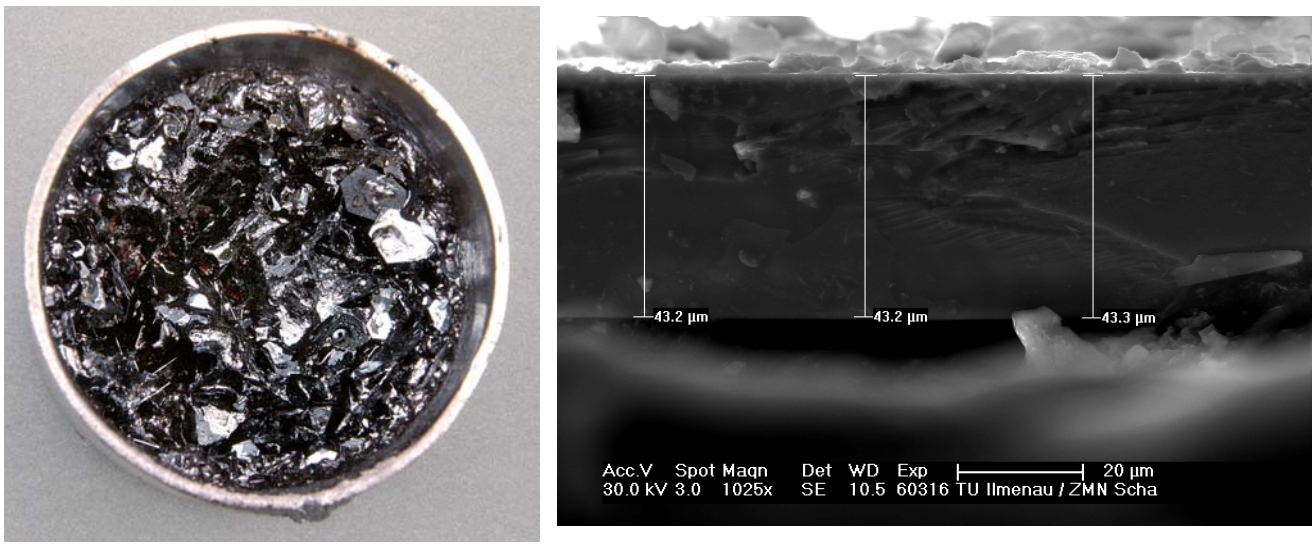

Figure 6 Sample Ha3
left side: crystallization on wall and bottom of crucible (diameter of crucible 40 mm)
right side: thickness measuring on a separated large crystal from the crucible

Figure 7 gives an impression of melt HaFe5 and figure 10 shows the XRD anaysis through the cross-section. The surface is made of BHF crystals which are orientated

in the crystallographic [001]-direction. Within the melt there are large BHF crystals without apparent alignment too. The grey, shiny crystals in figure 7 are these BHF crystals. The enclosing matrix seems visually amorph. However, in the middle of the drilling core hematite could be detected with low intensities.

Fig. 7 Sample HaFe5

top left: large BHF crystals on the surface of the solidified melt

bottom left: fragment of the drilling core with circular drilling marks, unevenly spread large BHF crystals and brown segregation

bottom right: grinded and polished fragment, matrix nerved by cracks

A part of the larger crystals could be separated from samples Ha3, HaFe5 and HaFe8. In figure 8 you can see three crystals from sample HaFe5. They have edge length in the square direction of approximately 2 to 5 mm and their thickness is between 0.3 and 0.6 mm.

Figure 8 shows conglomerates of separated BHF crystals from sample HaFe5. Their edges length is between 20 and 200 µm and their thickness ranges between 100 and 300 nm. It is possible, that these small crystals did not directly crystallize in the melt, or at least not all of them. Figure 7 also shows exemplarily a crystal piece in which the

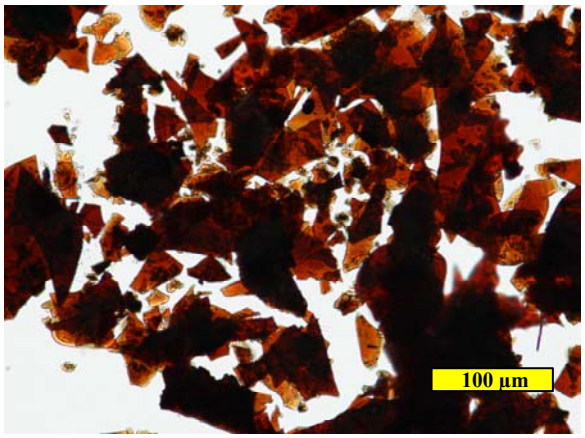

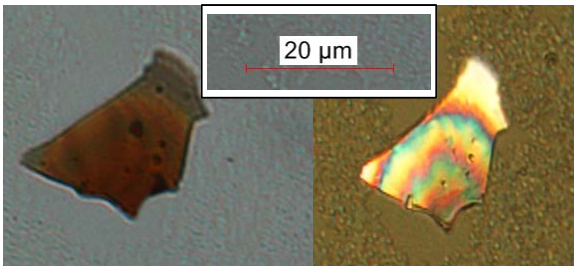

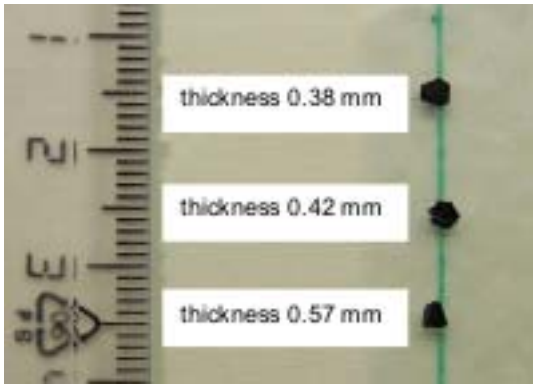

Fig. 8 Sample HaFe5

top left: small, transparent BHF crystals

bottom left: fragment of a crystal with incident and polarized light

bottom right: separated single crystals with millimetre size

the remaining tension is made visible by polarized light. The geometry shows that this crystal was a part of larger original crystal. In our opinion this could have happened because of mechanical inpacts while the preparation and the chemical separation.

3.3 Structural Analysis

To ascertain the crystalline phases and the crystal structure of the solidified material after the melting process, X-ray diffraction with the Bragg-Brentano-method [7] and nickel filtered copper-radiation were carried out with an X-ray diffractometer D5000.

For rating the crystallization on the surface of the solidified melts, differences were noticed in the development of the structure. The crystals at the separated surface of sample Ha3 and the crystals at the solidified surface of samples HaFe5 and HaFe8 are BHF single crystals. Figure 9 shows the XRD analyses for these samples.

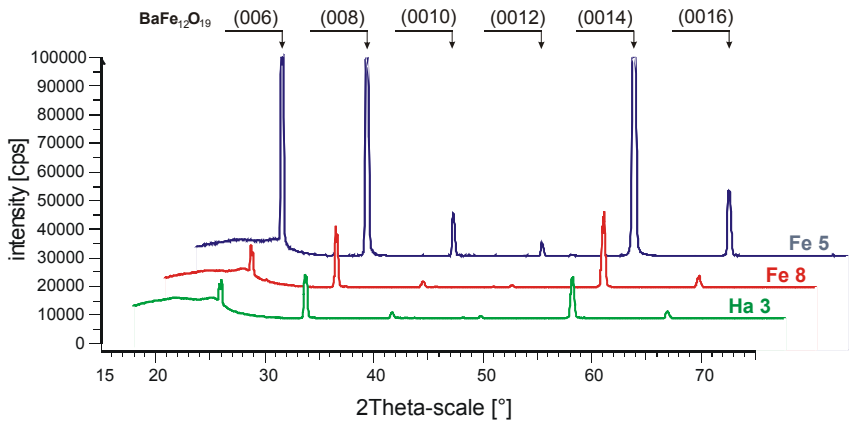

Figure 9

XRD analyses; top scans from different samples

(Peaks from $BaFe_{12}O_{19}$ only)

While in samples Ha3 the crystals are disorientated (see figure 6) only minor intensities were detected. In sample HaFe5 a perfect alignment of the bariumhexaferrite to the surface can be seen. The multitude of repeating interferences in the diffraction diagram is caused by {002}-pole and confirms the alignment of bariumhexaferrite perpendicularly to the surface. Other crystal phases could not be detected on the surfaces of the samples.

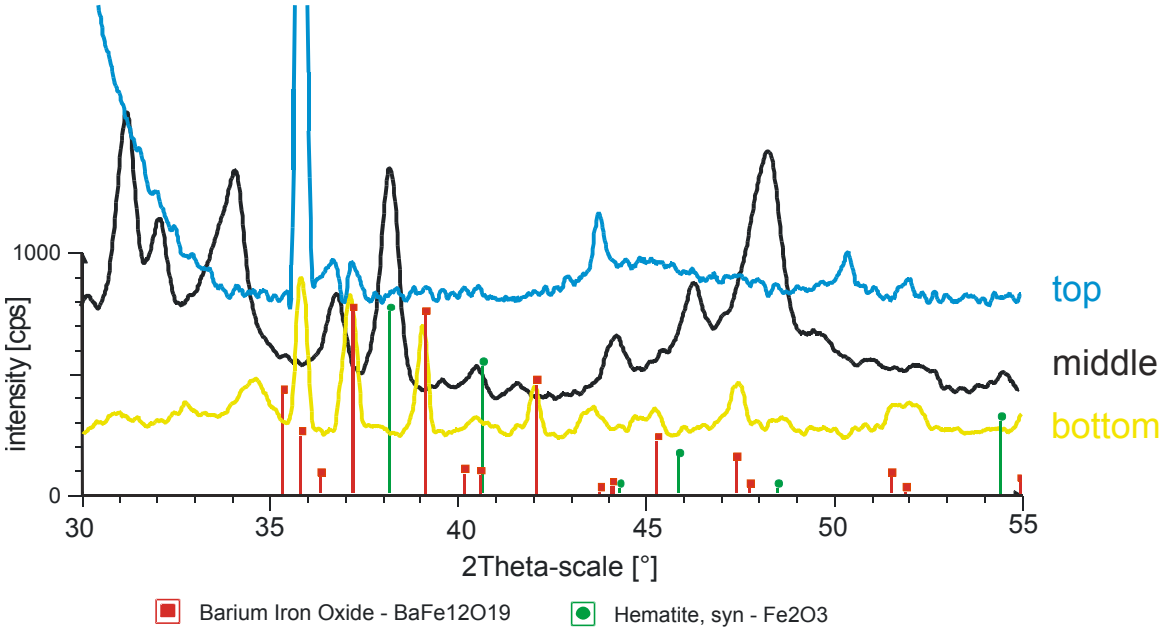

Figure 10 XRD analyses of the samples HaFe5 on solid material

Figure 10 shows the analyses of the crystals grown on the profile from top to bottom. On the surface of the drilling core (top), there is the single-crystalline phase of the bariumhexaferrite only. The bottom side, however, shows a polycrystalline structure of the hexagonal phase $BaFe_{12}O_{19}$. Even the rhombohedral Fe_2O_3 is part of the

structure and was detected in the middle of the drilling core. The peaks for 2Theta < 32° in the middle could not be identified. Presumably these phases are types of crystals with other Fe_2O_3- and BaO-contents. The crystalline phases of the $Ba_2Fe_6O_{11}$ and of the $Ba_5Fe_2O_8$ could not be detected definitely.

The orientation within a poly-crystal does not always have to be distributed without order like it would be in a powder. Due to the melting process with temperatures at around 1,200 °C and the streaming conditions within the melt no orderless orientation has taken place but the crystals feature a preference orientation.

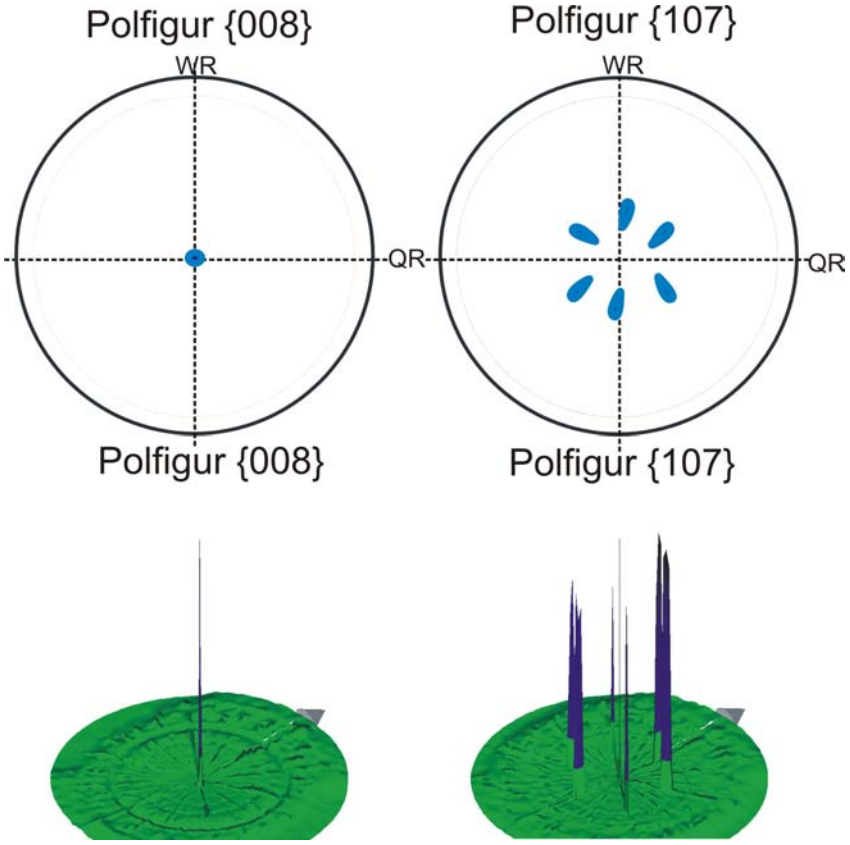

Figure 11

Pole-figures of a BHF single crystal of the samples HaFe5

The orientation's specification of a crystal describes the position of the crystallographic axes. From the surface area of sample HaFe5 a few single crystals of the hexagonal phase $BaFe_{12}O_{19}$ were separated. To qualify the orientation pole-figures were taken by an X-ray diffractometer [7]. The orientation of the bariumhexaferrite crystals was already found with the Bragg-Brentano-method (see figure 9). Only the pole-figure of plane {002} and the therewith connected alignment of [001] perpendicular to the sample's surface could be determined. Figure 11 shows the most intensive pole-figure, the plane {008}. Figure 11 also shows the pole-figure for plane {107}, which effects the most intensive interference of a polycrystalline $BaFe_{12}O_{19}$. In

the analyses of the separated crystals this interference did not observed and so the structure was confirmed as single crystal definitely.

The results of the structure analyses can be authenticated by X-ray fluorescence (XRF). Table 2 shows results of the measurement of chemical composition of six large crystals, taken from sample HaFe5 and compared to values of ideal BHF.

Table 2 XRF analyses of large crystals from sample HaFe5

sample code	measured concentration in ma%		oxidic concentration in ma%	
	Fe	Ba	Fe_2O_3	BaO
HaFe5-gK	83.9	16.1	86.97	13.03
HaFe5-mK	84.2	15.8	87.22	12.78
HaFe5-kK	84.0	16.0	87.05	12.95
HaFe5-K38	84.0	16.0	87.05	12.95
HaFe5-K42	84.2	15.8	87.22	12.78
HaFe5-K57	84.0	16.0	87.05	12.95
mean value			87.09	12.91
$BaFe_{12}O_{19}$ theoretically			86.20	13.80

All analysed crystals feature an enhanced Fe_2O_3 concentration, which is between 0.8 and 1.0 ma% higher than the theoretical concentration.

Figure 12 shows the XRD analyses of all samples and comparatively one from sample Ha-N. In all analyses dissolved powder with grain sizes smaller than 63 µm was examined. The crystalline material in all samples was $BaFe_{12}O_{19}$.

The samples partly feature a very strong orientation, similar to the crystals from the surface. Orientation in this case means that the sample material arranged itself on the sample carrier, so that the c-axis of the crystals is pointing towards the X-ray detector. Reasons for the orientation are the crystals' appearances as single crystals on the one hand and their laminar extension in a- and b-direction on the other one. Ha3 and HaFe4 feature the strongest orientation, which is to be identified on the basis of the large peaks at 26,74° and 35,922°. Both samples were tempered at a temperature

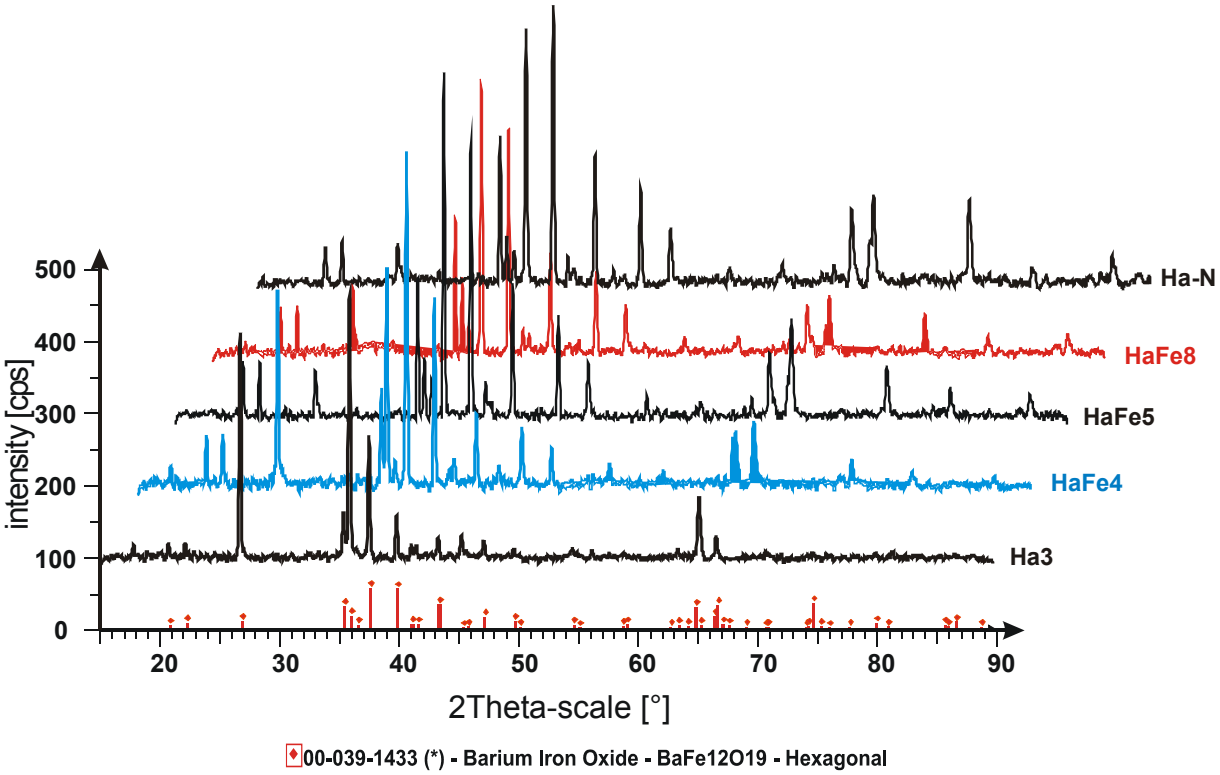

Figure 12 XRD powder diffraction for dissolved crystals for different samples

range between 1,200 and 1,100 °C. Increasing the duration of tempering causes less orientation, which can be seen on sample HaFe4. In this sample the main peak of BHF at 35,510° features the highest intensity again.

During longer tempering and coeval sinking temperature the orientation decreases and all peaks of reference-file 039-1433 can be verified. In comparison to Ha-N, a BHF made after the glass crystallization technique, there are only differences with the peaks intensities at 32.149° and 34.090°.

It is noticeable, that with growing tempering duration the texture decreases, which means that the relation between area and thickness of the crystals changes for the benefit of the thickness. From this it follows, that BHF-crystals grow within a melt as flat structures with preference in the a-b-axis and grow in thickness (c-axis) with increasing duration.

XRD analyses on flakes of sample K3 and on frits of Ha3 and HaFe4 showed no evaluable peaks. These samples are amorphous with XRD.

3.4 Magnetic Properties

The measuring of magnetic properties were accomplished within a vibration magnetometer (VSM) Modell 290 of Princeton Measurement Corp. To calibrate the device a Ni-foil with a magnetic moment of 51.67 memu was used. The maximum of the field applied during the measurement was 1,273 kA/m (16,000 Oe). This field is adequate, because the hysteresis curve has already been closed again for smaller field intensities and the increase of the magnetic moment is a marginal one only. A measurement of the coercive field force $_jH_c$ and of the remanence M_r was carried out. The saturation magnetization M_s was calculated by an internal programme of VSM.

Table 3 shows the analysed samples and results. Sample K3-N acts as a reference sample for magnetic properties. The sample is amorphous and no crystallites were detected in it [8]. The straight line in figure 13 shows analogical paramagnetic behaviour. By analysing this result more accurately, rudimentary ferromagnetic properties can be found in this untempered glass.

Table 3 Overview over samples, tempering duration, magnetic features and density

sample code	remarks	time min	$_jH_c$ kA/m	M_r emu/g	M_s emu/g	density g/cm³
K3-N	crushed flakes – reference sample (X-ray amorphous glass)	0	30.23	0.02	0.30*	4,2406
Ha3-F	residuum from separated frit	303	30.30	0.83	6.54*	n.m.
Ha3	separated BHF crystals	303	17.61	3.97	65.88	5.2390
HaFe4	separated BHF crystals	1,000	30.06	7.15	59,42	5.2660
HaFe5	separated BHF crystals	4,000	22.80	10.48	64.94	5.2845
HaFe8	separated BHF crystals	8,000	78.66	12.95	66.10	5.2890
Ha-N	separated BHF crystals (glass crystallization technique)	1,800 (850°C)	419.77	35.72	64.30	5.3090
BHF-H	ceramic BHF powder	0	213.90	34.98	64.03	n.m.
SHF-H	ceramic strontium hexaferrite powder	0	268.65	34.06	54.58	n.m.

* values only represent the spec. magnetic moment at 1270 kA/m not the real saturation M_s

Through defined cooling from 1,200 °C the whole melt changes structurally. In the separated residuum in the melt of sample Ha3 (code: Ha3-F) the coercive field force, which is already known from glass, can be measured, although with a significant higher remanence. For other large crystals segregated from the melt and for all other

separated crystals ferromagnetic behaviour can be detected. In figure 12 a few characteristic curves are given.

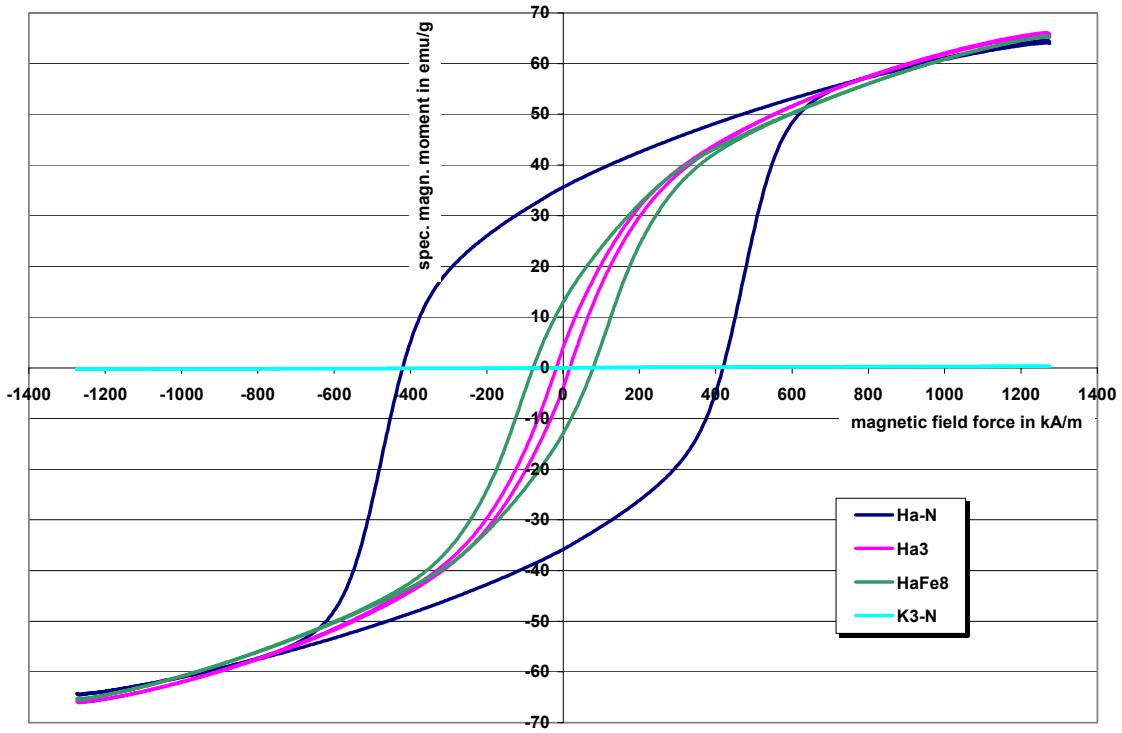

Figure 13 Hysteresis curves for different samples

The magnetic properties of the samples Ha3 and HaFe5 are situated within the top border area of common soft magnetically materials. The values of ${}_jH_c$ and M_r rise with increasing tempering duration and simultaneously decreasing temperature, while the saturation magnetization is about 65 emu/g. If this value is reached, the presence of BHF can be assumed. This conclusion is also supported by the XRD and XRF analyses.

In figure 14 coercive field force, remanence and density are illustrated in relation to the tempering duration. For durations $\geq$ 300 min the increase of density is low, but the increase of remanence stays significant. The coercive field force of BHF crystals rises from 17.6 up to 78.6 kA/m. However, the coercive field force acts in a very sensitive way (see values at 1,000 min; sample HaFe4) und might be used as a kind of quality criterion. For this tempering duration HaFe4 features a comparatively high

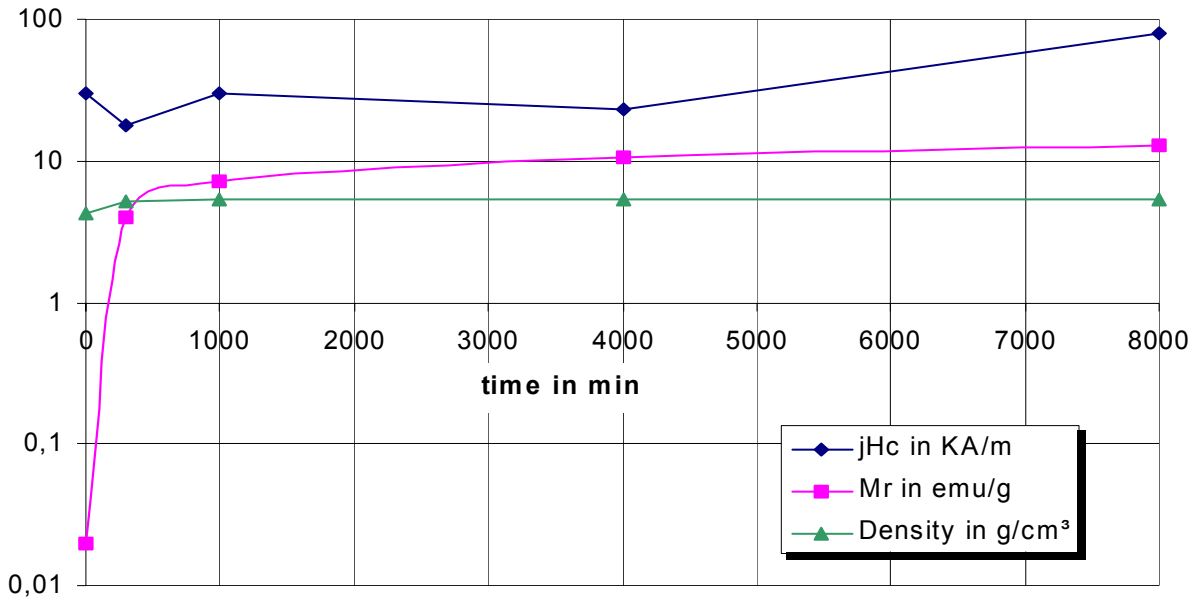

Figure 14 Dependences of coercive field force ${}_jH_c$, remanence M_r and density from the tempering duration

${}_jH_c$ with a relatively low M_r. Contaminations on the BHF crystals from rests of borate can be the reason for that, since no further crystal phases could be detected (see XRD in figure 12). It is remarkable, that in the lower temperature area, between 800 and 400 °C the remanence increases up to 100% and the coercive field force increases more than 100%.

Furthermore magnetic properties in relation to the temperature were measured from samples Ha-N and HaFe5. Figure 15 shows those relations for the coercive field force, for the specific magnetic moment and the remanence at an applied field force of 1,114 kA/m (14,000 Oe). The changes of all properties are very clear to be seen within the range of the Curie point at about 450 °C.

The specific magnetic moments of both samples are equal at room temperature and have an almost identical dependence. The remanence was illustrated as far as 450 °C, because there is paramagnetic behaviour at higher temperatures. In contrast to sample Ha-N, which features continuously dropping values from 35 (20 °C) to 3.8 emu/g, the remanence of HaFe5 stays constantly at about 7 emu/g up to 400 °C. Only after that process there is a significant drop to 1.8 emu/g at 450 °C.

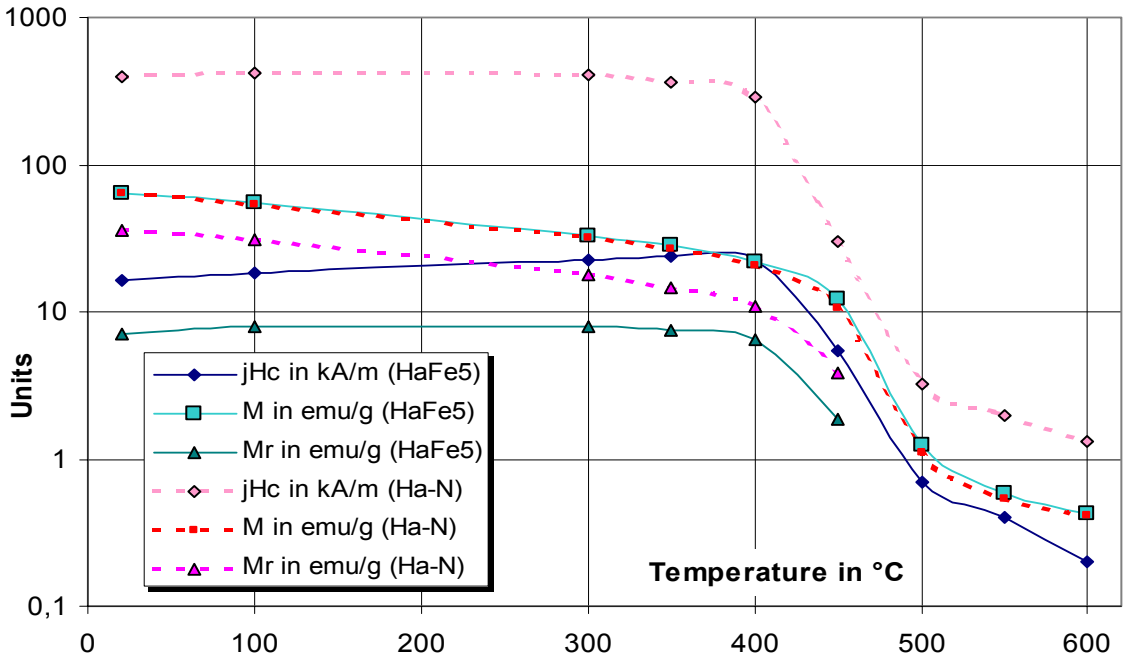

Figure 15 Dependences on temperature of coercive field force ${}_jH_c$, specific magnetizing M and remanence M_r for the samples HaFe5 and Ha-N

The results of the coercive field force differ, too. At room temperature, the value for sample Ha-N is, with a value of 400 kA/m, 20 times higher. At 300 °C a decrease of coercive field force takes place (400 °C: 285 kA/m → 450 °C: 30 kA/m). The coercive field force of sample HaFe5 is at room temperature 16 kA/m. In opposite to sample Ha-N sample Hafe5 shows an increase up to 400 °C (23 kA/m). Below 450 °C it drops to 5.4 kA/m.

4. Evaluation of Results

The presented results show, that for the investigated material 39.6 mol% BaO, 35.4 mol% B_2O_3 and 25 mol% Fe_2O_3 crystallization of BHF can be achieved through defined cooling of the melt. Related to the tempering conditions magnetic properties can be adjusted. They are between already known soft magnetic materials and hard magnetic ferrites.

We observed an orientation of the investigated BHF crystals on the surface of the melt but not in the melt itself. The reason is probably the low magnetic properties (coercive field force and remanence) at the crystallisation temperatures above the

Curie point. So, we can be made no statement on the interaction between the used magnetic DC field and the BHF crystals in the melts. At this time we assume, that there are significant interactions between the thermal induced streaming of the electrically conductiv melt in the crucible and the magnetic field.

The grown BHF crystals are single crystals and have dimensions up to 5 mm in length. The thickness is a function of tempering duration. Such crystals have not been available yet. It is well imaginable, that they are applicable not only in magnetic engineering. We propose for manufacturing such crystals flat crucibles with wide-spread surfaces. Because of this geometry more-than-average and completely shaped crystals can be obtained.

The authors will continue in dealing with these large crystals and in determining their mechanical properties. Another publication is intended, which includes these results, as well as results on crystallization without the DC magnetic field.

Acknowledgement

The authors would like to thank their fellows from the Junior Research Group “Electromagnetic Processing of Materials” (EPM) for their all-embracing support and professional consulting. We also want to thank the “Zentrum für Mikro- und Nanotechnologien” (ZMN) as well as to the departments „Glas- und Keramik-technologie“ and „Werkstoffe der Elektrotechnik“ especially to Dr Chr. Georgie (XRD) and to Dr V. Bretternitz (XRF).

Sincerce thanks are given to Dr R. Müller from IPHT e.V. in Jena for professional advice and for the measurement of magnetic properties.

EPM works until December 31st 2006 at the TU Ilmenau supported by the *Thüringer Ministerium für Wissenschaft, Forschung und Kunst* within the programme “Hochschul- und Wissenschaftsprogrammes zur Förderung innovativer Forschungs-strukturen in den neuen Ländern und Berlin“.

References

[1] Ertel-Ingrisch, W., Hartmann, K., Ludwig, I., Weih, P.: Crystallisation Inside High Magnetiv DC Fields, 50. Intern. Wiss. Kolloq., Ilmenau, Sept. 2005
[2] Jurisch, F.: Entwicklungen auf dem Permanentmagnetmarkt.- 14. Kleinmaschinenkolloquium: TU Ilmenau, März 2006
[3] Knauf, O.: Nutzung großer Abkühlgeschwindigkeiten zum Amorphisieren spontan kristallisierender oxidischer Schmelzen, dargelegt am System BaO-Fe2O3-B2O3, Habilitation, Ilmenau, 1988
[4] Haberey, F.: Preparation of M- and W-type hexaferrite particles by the glass crystallsation mathod on the basis of the pseudo-ternary system Fe2O3-BaO-B2O3; IEEE Transactions on Magnetics, Vol. Mag-23, No 1, Jan. 1987
[5] Hamann, B., Lohse, U., Ertel-Ingrisch, W., Kraffert, C.: Experimentiereinrichtung für Kristallisation bei hohen Temperaturen im starken magnetischen Gleichfeld.- elektrowärme international, Heft 2, Jun 2006
[6] Brandes, Ria: Recycling der Abprodukte des Herstellungsprozesses von Feinpulvern nach der Glaskristallisationstechnik; Dissertation, Ilmenau, 2000
[7] Spieß, L., Schwarzer, R., Behnken, H., Teichert, G.: Moderne Röntgenbeugung, Teubner, Wiesbaden, 2005
[8] Schadewald, U.: Untersuchung zur bottom-up-Kristallisation von modifizierten Bariumhexaferritpulvern; Diplomarbeit, Ilmenau, 2005

Authors:

Dr.-Ing. Bernd Hamann
TU Ilmenau, Fak. EI, FG Elektrothermische Energiewandlung, EPM
D-98693 Ilmenau
Phone: +49-3677-692877
Fax: +49-3677-691552
E-mail: bernd.hamann@tu-Ilmenau.de

Dipl.-Ing. Jens Schawohl
TU Ilmenau, Fak. EI, FG Werkstoffe der ET
D-98693 Ilmenau
Phone: +49-3677-693403
Fax: +49-3677-693353
E-mail: jens.schawohl@tu-Ilmenau.de

Dipl.-Chem. Cornelia Kraffert
TU Ilmenau, Fak. EI, FG Elektrothermische Energiewandlung, EPM
D-98693 Ilmenau
Phone: +49-3677-691505
Fax: +49-3677-691552
E-mail: cornelia.kraffert@tu-Ilmenau.de